PLOS Computational Biology

RESEARCH ARTICLE

A kinetic model for USP14 regulated substrate degradation in 26S proteasome

Di Wu[1], Qi Ouyang[1,2,3], Hongli Wang[1,2]*, Youdong Mao[1,2,4,5,6]*

1 The State Key Laboratory for Artificial Microstructures and Mesoscopic Physics, School of Physics, Peking University, Beijing, China, **2** Center for Quantitative Biology, Peking University, Beijing, China, **3** School of Physics, Zhejiang University, Hangzhou, China, **4** Peking-Tsinghua Center for Life Sciences, Peking University, Beijing, China, **5** National Biomedical Imaging Center, Peking University, Beijing, China, **6** AI for Science (AI4S)-Preferred Program, School of Chemical Biology and Biotechnology, Peking University Shenzhen Graduate School, Shenzhen, China

* hlwang@pku.edu.cn (HW), ymao@pku.edu.cn (YM)

OPEN ACCESS

Citation: Wu D, Ouyang Q, Wang H, Mao Y (2025) A kinetic model for USP14 regulated substrate degradation in 26S proteasome. PLoS Comput Biol 21(5): e1012761. https://doi.org/10.1371/journal.pcbi.1012761

Editor: Changbong Hyeon, Korea Institute for Advanced Study, KOREA, REPUBLIC OF

Received: December 31, 2024

Accepted: March 17, 2025

Published: May 2, 2025

Data availability statement: The source code and data used to produce the results and analyses in this manuscript are available on GitHub at https://github.com/diwu31415/USP14_proteasome

Funding: This work was supported by the National Natural Science Foundation of China (12090051 to HW; 12125401 to YM), the

Abstract

Despite high-resolution structural studies on the USP14-proteasome-substrate complexes, time-resolved cryo-electron microscopy (cryo-EM) results on USP14-regulated allostery of the 26S proteasome are still very limited and a quantitative understanding of substrate degradation dynamics remains elusive. In this study, we propose a mean field model of ordinary differential equations (ODEs) for USP14 regulated substrate degradation in 26S proteasome. The kinetic model incorporates recent cryo-EM findings on the allostery of 26S proteasome and generates results in good agreement with time-resolved experimental observations. The model elucidates that USP14 typically reduces the substrate degradation rate and reveals the functional dependence of this rate on the concentrations of substrate and adenosine triphosphate (ATP). The half-maximal effective concentration (EC50) of the substrate for different ATP concentrations is predicted. When multiple substrates are present, the model suggests that substrates that are easier to insert into the OB-ring and disengage from the proteasome, or less likely to undergo deubiquitination would be more favored to be degraded by the USP14-bound proteasome. The mean field model proposed here quantitatively considers the process of proteasomal substrate degradation from the perspective of chemical kinetics, and provides a quantitative framework to decode the dynamic interplay between USP14 and the proteasome.

Author summary

The proteasome is a crucial protein complex involved in the degradation of damaged or unnecessary proteins within cells, requiring ATP and ubiquitin for its functioning. It is regulated by cellular factors that transiently associate with it,

PLOS Computational Biology

National Key Research and Development Program of China (2023YFF1204400, and 2023YFF1204401 to YM), the Starry Night Science Fund of Zhejiang University Shanghai Institute for Advanced Study (to QO), and AI for Science (AI4S)-Preferred Program, Peking University Shenzhen Graduate School (to YM). The funders had no role in study design, data collection and analysis, decision to publish, or preparation of the manuscript.

Competing interests: The authors have declared that no competing interests exist.

often referred to as proteasome-associated proteins. USP14 is such a protein that activates its deubiquitination activity through reversible binding to the proteasome, thereby decreasing the substrate degradation activity of the proteasome. In this study, we developed a kinetic model to describe how USP14 regulates substrate degradation in proteasome based on recent experimental findings. The model yields result consistent with experimental observations, demonstrating that the mean-field description of mass action law for chemical reactions also applies to complex biomolecular machineries.

1. Introduction

The proteasome is the core of the ubiquitin-proteasome system (UPS) in eukaryotes, playing a pivotal role in regulating protein degradation processes [1,2]. It is a 2.5-megadalton protein complex composed of core particle (CP) and regulatory particle (RP) [3]. Substrate proteins tagged with ubiquitin are recognized by ubiquitin recognition sites on RPN1 subunit, deubiquitinated by the subunit and unfolded by ATPase motor, translocated into the CP, and ultimately degraded into short peptides at the hydrolytic sites within CP. Previous studies have elucidated the dynamics of the proteasome through various experimental approaches, including mutagenesis experiments [4,5], single-molecule experiments [6,7], and cryo-electron microscopy (cryo-EM) experiments [3,8–10]. In vivo, the function of the proteasome is regulated by cellular factors that transiently associate with it, often referred to as proteasome-associated proteins [11–13]. These include the ubiquitin-specific protease 14 (USP14) [14], deubiquitinating enzyme UCH37 [15–17], E3 ubiquitin ligase UBE3C/Hul5 [18,19], parkin [20], UBE3A/E6AP [21,22], etc. The enzymes interact directly or indirectly with the proteasome and thereby regulate its function. Among these enzymes, the structure and function of USP14 have been the focus of previous studies [14,19,23–27].

USP14 (or its homolog UBP6 in yeast) is a deubiquitinating enzyme that activates its deubiquitination activity by reversible binding to the proteasome, thereby regulating the UPS system [14]. Biochemical experiments have shown that USP14 can decrease substrate degradation activity of the proteasome [23,25]. Deletion of UBP6 in yeasts can leads to growth deficiencies [19]. Cryo-EM experiments have further studied how USP14/UBP6 binds to the proteasome and modulates its function [24,26,27]. USP14/UBP6 binds to the T2 site on the proteasomal regulatory particle non-ATPase (RPN) 1 via its ubiquitin-like (UBL) domain [28] and cleaves the ubiquitin chains through its ubiquitin-specific protease (USP) domain [25]. Recent time-resolved cryo-EM experiments have identified 13 distinct high-resolution structures of UPS14-bound proteasome and their temporal changes, providing a rough outline of transitions between these complexes [27]. While cryo-EM experiments with temporal resolution on USP14-regulated allostery of the 26S proteasome are very limited and remain a significant challenge, an accurate and quantitative understanding of substrate degradation dynamics is elusive. So far, no modeling studies have been reported regarding the dynamics of proteasomal substrate degradation regulated by USP14.

In this paper, we propose a kinetic model of ordinary differential equations (ODEs) based on recent experimental findings on the regulatory interactions between USP14 and the 26S proteasome during substrate degradation. The model well explains the recent experimental observations on the temporal changes in the distribution of human 26S proteasomal conformations [27]. In consistency with experimental observations, the model illustrates that the proteasome decreases its substrate degradation rate upon the regulation of USP14. Subsequent analyses with simplified models predict how the rate depends functionally on the concentrations of substrate and adenosine triphosphate (ATP), and the substrate's half-maximal effective concentration (EC50) across a wide range of ATP concentrations. In our model for multiple substrates, USP14 alters the proteasome's selectivity towards different substrates. Model results predict that the USP14-bound proteasome preferentially degrades substrates that readily access the OB-ring, are easier to detach from the proteasome, and are less prone to deubiquitination. The mean field model introduced here quantitatively examines proteasomal substrate degradation through the viewpoint of chemical kinetics, offering a framework to decipher the dynamic interaction between USP14 and the proteasome. The coarse-grained kinetic description of proteasome degradation dynamics is significant for both interpreting the existing experimental results and guiding future experimental studies with kinetic insights. Given the technical complexities associated with time-resolved cryo-EM investigations of proteasomal allostery, the theoretical model results are significant in achieving a deeper insight into the intricate process of proteasomal substrate degradation.

2. Results

2.1 Kinetic model of USP14-regulated proteasomal degradation of substrate

2.1.1 Experimental findings on the human 26S proteasomal conformations. In eukaryotes, the 26S proteasome serves as a central player in the complex process of degradation of proteins. USP14, a ubiquitin-specific protease acting as a deubiquitinating enzyme, binds to the proteasome in a reversible manner, thereby modulating the process of substrate degradation. The cartoon in Fig 1A illustrates the structure of 26S proteasome that are bound with USP14. For more details, we recommend referring to references [3,9,27]. As shown in Fig 1A, USP14 consists of two domains, namely UBL domain and USP domain. The UBL domain resembles the structure of ubiquitin and can bind to the T2 site of RPN1 in the proteasome. The USP domain possesses the capability of deubiquitination and contacts the exterior of the OB-ring opposite RPN11. The OB-ring forms the entrance of the polypeptide substrate into the ATPase motor and CP. The substrate is unfolded and translocated by the ATPase motor, and hydrolyzed within the CP.

Fig 1B summarizes the recent experimental findings on the human 26S proteasomal conformations and transitions during substrate degradation [3,9,27]. Four distinct proteasomal conformations (S_A, S_B, S_C, S_D) in the absence of both substrate and USP14 have been identified [9], and four types of conformations (E_A, E_B, $E_{C1,C2}$, $E_{D1,D2}$) in the presence of substrate have been recognized for the USP14-free proteasome [3]. Specifically, the substrate is not yet bound to the proteasome in E_A (identical to S_A), and is bound to the proteasome via the ubiquitin chain in E_B (without its N- or C-terminus being inserted into the ATPase motor of the proteasome). In E_C, the substrate is inserted into the ATPase motor and deubiquitinated by RPN11. It is subsequently translocated by the ATPase motor into the CP and hydrolyzed in E_D. The S_B, S_C, S_D conformations have similar structures to E_B, E_C, E_D, respectively, despite the absence of substrate [2,9].

For substrate degradation in 26S proteasome that is regulated by USP14, recent time-resolved cryo-EM experiments have disclosed a qualitative picture for proteasomal conformations and their temporal changes [27]. As illustrated with dashed boxes in Fig 1B, the recently observed 13 conformations of USP14-bound proteasome were categorized into E_A-like (E_{A1}^{UBL}, $E_{A2.0}^{UBL}$, $E_{A2.1}^{UBL}$), E_D-like (E_{D0}^{USP14}, E_{D1}^{USP14}, $E_{D2.0}^{USP14}$, $E_{D2.1}^{USP14}$, E_{D4}^{USP14}, E_{D5}^{USP14}), and S_D-like (S_B^{USP14}, S_C^{USP14}, S_{D4}^{USP14}, S_{D5}^{USP14}) classes. The E_A-like, E_D-like, and S_D-like conformations have structures similar to E_A, E_D, and S_D, which are not regulated by USP14. For more detailed information on the conformational difference in E_A-like, E_D-like, and S_D-like proteasomal states, please refer to the description in Supporting information. As indicated with thick gray links in Fig 1B, transitions

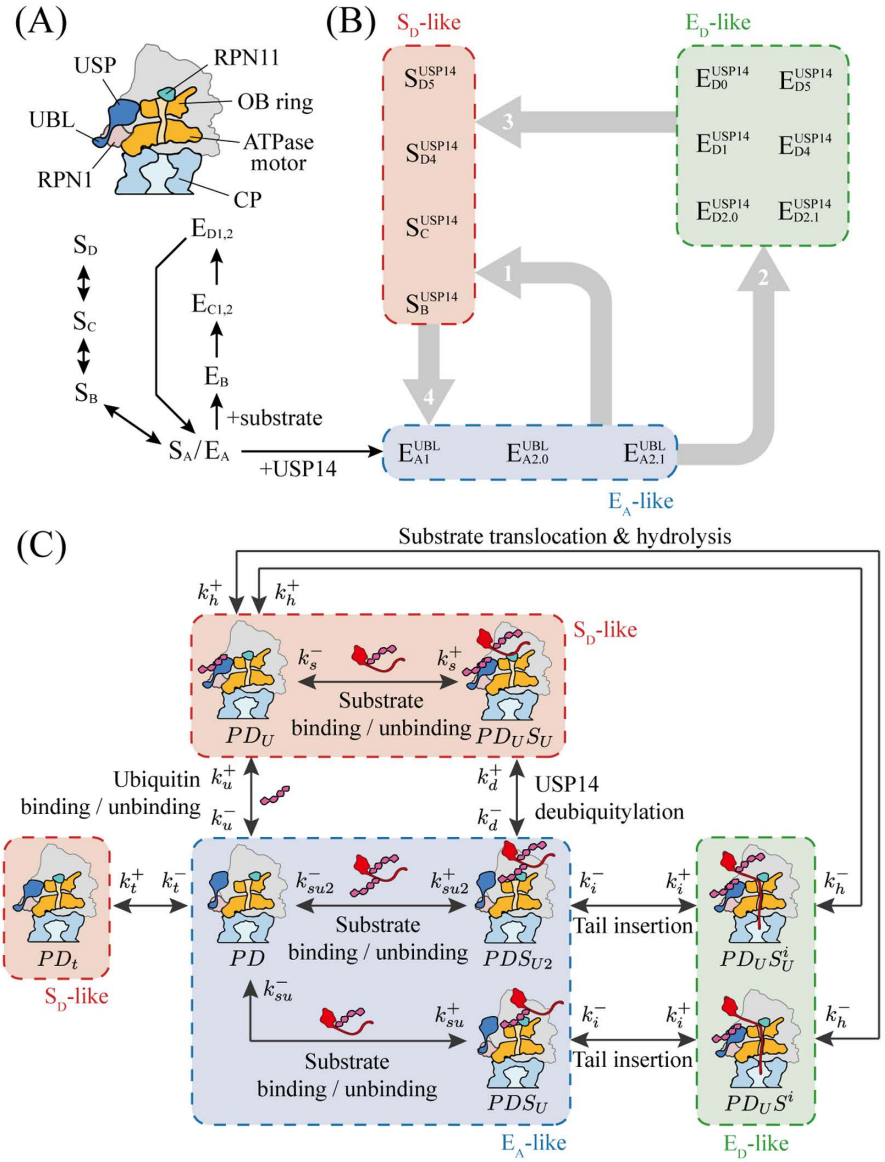

Fig 1. USP14-bound 26S proteasome in substrate degradation. (A) The structure of USP14-bound proteasome. (B) Conformations of the human 26S proteasome and their transitions known from experiments [3,9,27]. S_A, S_B, S_C, S_D (E_A, E_B, $E_{C1,C2}$, $E_{D1,D2}$) are for proteasomal conformations free of substrate (in the presence of substrate), with subscripts *A*, *B*, *C*, *D* (and the numbers) representing conformational (and sub-conformational) differences. The E_A-like, E_D-like, and S_D-like conformations shown in dashed boxes are for USP14-bound proteasome, with structures similar to E_A, E_D, and S_D. The superscript *UBL* (or USP14) denotes that the proteasome is bound with the UBL domain (or with both UBL and USP domains of USP14). The thin arrows (or thick gray arrows) are for experimentally certain (or less certain) conformation transitions. (C) The reaction network for USP14-regulated proteasomal substrate degradation reformulated from (B). Constituents of the proteasomal complex are denoted with *P* (for 26S proteasome), *D* (for USP14), and *S* (for substrates), respectively.

https://doi.org/10.1371/journal.pcbi.1012761.g001

occur among the E_A-like, S_D-like, and E_D-like conformations. Previous studies illustrated that in E_A-like conformations, competition exists between the deubiquitination of USP14 and the tail insertion of substrate [25]. The substrate could not be stably bound to the proteasome if the substrate ubiquitin is removed by USP14 before the tail insertion completes. This can make E_A-like states change into the S_D-like conformations (indicated by gray arrow 1 in Fig 1B). Conversely, if

ubiquitin is cleaved after tail insertion, the substrate can maintain a stable binding due to the force exerted by ATPase motor, facilitating subsequent unfolding and degradation processes, *i.e.*, E_A-like changes to E_D-like (refer to gray arrow 2 in Fig 1B). After the completion of substrate hydrolysis, the proteasome in E_D-like conformations returns to the unengaged S_D-like conformations [29], as denoted by gray arrow 3 in Fig 1B. Ultimately, the proteasome in the substrate-resistant S_D-like conformations changes back to the E_A-like conformations (refer to gray arrow 4 in Fig 1B).

2.1.2 Reaction network and kinetic model for USP14-regulated proteasomal substrate degradation. Based on the experimental findings as in Fig 1B, we sought to construct a reaction network for USP14-regulated E_A-like, E_D-like, or S_D-like conformations in substrate degradation (Fig 1C). In our model, the 13 distinct conformations are not considered directly as variables but are classified according to their differences and changes in the constituents of the complex. To account for conformational changes of the proteasome, the primary components of the complex are represented by the symbols *P* for the 26S proteasome, *D* for USP14, and *S* for substrates. For instances, the combination *PD* represents the 26S proteasome bounded with USP14, and *PDS* denotes the proteasome-USP14-substrate complex. For simplicity, the conformational differences in the ATPase motor are ignored in our model, and the proteasomal complex is characterized by whether it is bound with the ubiquitin chain (denoted by subscript *U*) and whether the substrate is engaged with its initial tail inserted into the OB-ring of the proteasome (denoted by superscript *i*). For an instance, PD_U represents the proteasome-USP14 complex with USP14 bound with the ubiquitin chain. Partially deubiquitination is permitted in our model. S_{U2} represents the substrate not deubiquitinated by USP14, and partially deubiquitinated substrate by USP14 is denoted with S_U. Applying the above scheme, the E_A-like conformations E_{A1}^{UBL}, $E_{A2.0}^{UBL}$, $E_{A2.1}^{UBL}$ involved in the processes before tail insertion or deubiquitination are represented with PD, PDS_{U2}, PDS_U in our model. The six E_D-like conformations responsible for substrate translocation and degradation are casted briefly in two states $PD_US_U^i$ and PD_US^i. Similarly, the four S_D-like conformations, involved in translocation inhibition, are simplified into two states PD_US_U and PD_U. In Fig 1C, PD_t represents a state before the addition of substrate. It belongs to the S_D-like class which undergoes a reversible transition to the *PD* state in E_A-like type conformations in absence of substrate.

To take into account the experimental findings of conformational changes as illustrated in Fig 1B, state transitions occur in the simplified states in our model (refer to Fig 1C). Substrate binding/unbinding take place in the E_A-like states (PD, PDS_{U2}, PDS_U) and in the S_D-like states (PD_US_U, PD_U), thus cause transitions between the E_A-like and S_D-like states. Secondly, the E_A-like states PDS_{U2}, PDS_U can change into E_D-like states $PD_US_U^i$ and PD_US^i by tail insertion of substrate engagement. The accomplishment of substrate translocation and hydrolysis transforms the E_D-like states $PD_US_U^i$ and PD_US^i into the S_D-like state PD_U. In addition, the initial E_A-like state PD (or PDS_{U2}) can be converted to the S_D-like state PD_U (or PD_US_U) by ubiquitin binding (or deubiquitylation of USP14).

In our model, we assume that 26S proteasomes, USP14, and substrates are present in abundance and the reactions among them follow the mass action law. The chemical reaction dynamics for substrate degradation in 26S proteasome regulated by USP14 in Fig 1C can be described with eleven variables, eight of which represent the concentrations of E_A-like states (PD, PDS_{U2}, PDS_U), E_D-like ($PD_US_U^i$, PD_US^i), and S_D-like (PD_US_U, PD_U, PD_t) states for USP14-bound proteasome, two for the concentrations of substrates (S_{U2}, S_U), and one for the concentration of ubiquitin chain (U). The ordinary differential equations for the reactions are listed in Supporting information (Equations A in S1 Text). The parameter values of Equations A in S1 Text were determined by fitting the time-resolved cryo-EM experimental data [27]. Detailed information of fitting is given in Method.

2.1.3 The dynamics of USP14-bound proteasomal substrate degradation. The coupled ordinary differential equations (Equations A in S1 Text) for the kinetic model of USP14-regulated proteasomal substrate degradation have been numerically solved, and the results are presented in Fig 2. The time evolution in the proportions of E_A-like (PD, PDS_{U2}, PDS_U), E_D-like ($PD_US_U^i$, PD_US^i), and S_D-like (PD_US_U, PD_U, PD_t) conformations is readily obtained from the simulated dynamics of eight variables for USP14-bound proteasome concentrations, as illustrated in Fig 3A. The temporal change in the ratio of the residual substrate concentration (S_{U2}, S_U) relative to the initial amount is also shown. Upon

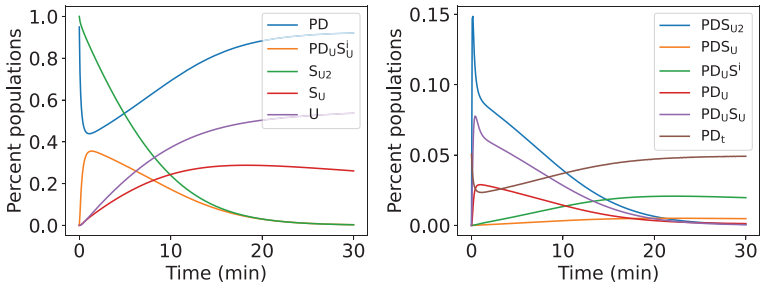

Fig 2. Time evolution for the reactions in Fig 1C for USP14-regulated proteasomal substrate degradation. The results are obtained by numerical simulations of Equations A in S1 Text. Detailed information of calculation is given in Method. The parameters used in simulation are listed in Supporting information (Table A in S1 Text).

https://doi.org/10.1371/journal.pcbi.1012761.g002

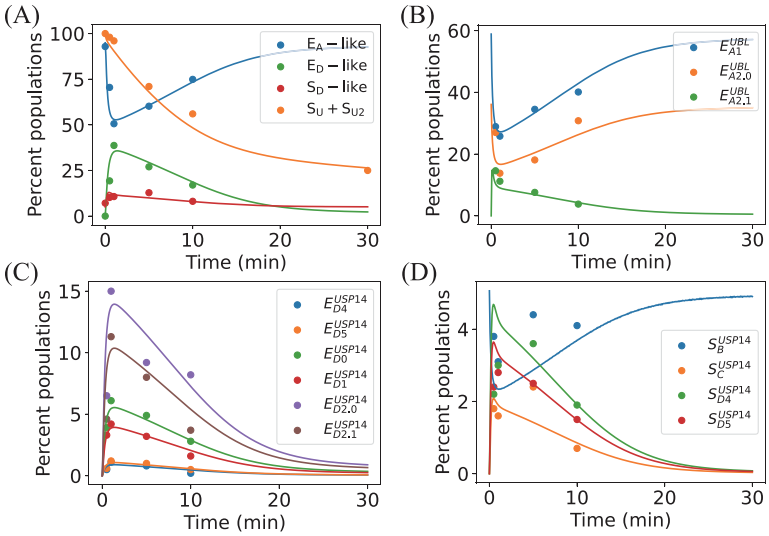

Fig 3. Dynamics of the USP14-bound proteasome. (A) Time evolution of the proportions of E_A-like, E_D-like, and S_D-like categories of conformation, as well as the concentration of residual substrate (S_{U2}, S_U) relative to the initial amount over time. (B) Temporal changes in the proportions of E^{UBL}_{A1}, $E^{UBL}_{A2.0}$, and $E^{UBL}_{A2.1}$ conformations within the E_A-like conformation. (C) Temporal changes in the proportions of E^{USP14}_{D0}, E^{USP14}_{D1}, $E^{USP14}_{D2.0}$, $E^{USP14}_{D2.1}$, E^{USP14}_{D4}, and E^{USP14}_{D5} conformations within the E_D-like conformation. (D) Temporal changes in the proportions of S^{USP14}_{B}, S^{USP14}_{C}, S^{USP14}_{D4}, and S^{USP14}_{D5} conformations within the S_D-like conformation. Solid lines represent simulation results, and dots are from the experimental data [27].

https://doi.org/10.1371/journal.pcbi.1012761.g003

substrate addition at zero minute, the proportion of E_D-like conformations, which are involved in substrate engagement, translocation, and hydrolysis, increases rapidly in the first minute, and falls slowly from the peak value in the following thirty minutes. On the contrary, the proportion of E_A-like conformations, which are responsible for the processes before substrate tail insertion or deubiquitination, decreases rapidly to the bottom value and recovers slowly as the substrate is degraded. The two opposing trends arise naturally due to the conservation of the total proteasome concentration. The proportion of S_D-like conformations, which are associated with degradation inhibition mediated by ubiquitin-bound USP14, maintains at low percentages and has no prominent changes during degradation as the residual substrate concentration decreases continuously. At 30 minutes, there are approximately 25% of the substrate remained undegraded. Recent time-resolved cryo-electron microscopy (cryo-EM) experiments have elucidated the dynamic shifts in the proportions of 13 distinct conformational states as well as the progressive decrease in residual substrate levels over time [27]. These

experimental findings were obtained at a temperature of 10°C under specific conditions: 1 mM ATP, 10 μM substrate $Sic1^{PY}$, and 1 μM USP14-bound proteasome. As illustrated in Fig 3A, the model results (curves) agree closely with the experimental findings (the dots).

As the 13 intermediate conformations are not explicitly included in our model as dynamical variables (due to lack of detailed experimental information of conformational changes), the proportions and their dynamical changes cannot be directly obtained in our simulations. Based on reasonable assumptions, the experimentally observed changes in the proportions of 13 intermediate conformations can still be inferred in our model. Firstly, the six E_D-like conformations (E_{D0}^{USP14}, E_{D1}^{USP14}, $E_{D2.0}^{USP14}$, $E_{D2.1}^{USP14}$, E_{D4}^{USP14}, and E_{D5}^{USP14}) are involved primarily in fast changes of the ATPase motor during substrate unfolding and translocations. As they represent a series of intermediates changing much faster than the complete rounds of substrate translocation, the transitions between the six E_D-like conformations are effectively in quasi-equilibrium. It is reasonable to assume that the proportions of these six intermediates in the whole of E_D-like conformations are fixed during the substrate degradation. In our simulations, the fixed percentages are obtained by fitting the experimental results, which are 2.5% for E_{D4}^{USP14}, 3.0% for E_{D5}^{USP14}, 15.5% for E_{D0}^{USP14}, 11.0% for E_{D1}^{USP14}, 39.0% for $E_{D2.0}^{USP14}$, and 29.0% for $E_{D2.1}^{USP14}$, respectively. As shown in Fig 3C, the dynamical changes in the proportions of the six E_D-like conformations obtained from our simulations closely match the experimental data.

For the three E_A-like conformations, E_{A1}^{UBL} lacks any visible substrate, $E_{A2.0}^{UBL}$ shows ubiquitin bound at the RPN11, and $E_{A2.1}^{UBL}$ exhibits both ubiquitin and subtle substrate density on RPN11. Given the difficulty of cryo-EM in visualizing substrate conformations outside the OB-ring, we consider $E_{A2.1}^{UBL}$ to encompass both PDS_{U2} and PDS_U states in our model, *i.e.*, $[E_{A2.1}^{UBL}] = [PDS_{U2}] + [PDS_U]$. We hypothesize that $E_{A2.0}^{UBL}$ represents an unstable binding of ubiquitin (possibly originated in substrate-tagged ubiquitin chains or ubiquitin chains generated by USP14 deubiquitination). Considering the constant total number of ubiquitin chains in experiment, we assume that $E_{A2.0}^{UBL}$ maintains a rapid equilibrium with E_{A1}^{UBL} and corresponds concurrently to the *PD* state in the model. Thus, the percentages of E_{A1}^{UBL} and $E_{A2.0}^{UBL}$ in the whole of *PD* conformation can be considered as fixed, which are similarly fitted to be 62.0% and 38.0%, respectively. The results in Fig 3B show that the model results are in good agreement with the experimental data.

The four S_D-like conformations primarily differ in the status of the *CP* gate and the conformation of the ATPase motor, making it challenging to establish a direct correspondence to our model based solely on their conformational features. In our simulations, we hypothesize that S_B^{USP14} directly corresponds to the PD_t state (*i.e.*, $[S_B^{USP14}] = [PD_t]$), and that S_C^{USP14}, S_{D4}^{USP14}, and S_{D5}^{USP14} correspond to the PD_US_U and PD_U states. Due to the reduced affinity between the substrate and the proteasome after USP14-mediated deubiquitination, cryo-EM images are likely unable to differentiate the PD_US_U and PD_U states. The transitions among S_C^{USP14}, S_{D4}^{USP14}, and S_{D5}^{USP14} may achieve rapid equilibrium. Their percentages in the whole of PD_US_U and PD_U are fixed, which have been fitted to be 20.5% (S_C^{USP14}), 45.0% (S_{D4}^{USP14}), and 35.0% (S_{D5}^{USP14}), respectively. In Fig 3D, the simulation results are also consistent with the experimental data for $S_C^{USP14}$and S_{D5}^{USP14}. The deviation between theory and experiment partially exists in $S_B^{USP14}$and S_{D4}^{USP14}. The inconsistency might be due to the relatively low proportions of S_B^{USP14} and S_{D4}^{USP14} conformations (less than 5% at maximum) in the total of 13 conformations, making the experimental measurements of their proportions more susceptible to measurement uncertainties.

2.2 Simplified model and the influence of USP14, substrate and ATP on substrate degradation

2.2.1 The effect of USP14 on substrate degradation rate. To check into the influence of USP14 on substrate degradation by the proteasome, we proceed with additional simplifications to the kinetic model that we have discussed above. Specifically, we neglect the more detailed PDS_U and PD_US^i states in Fig 1C and consider only the case where substrate not deubiquitinated by USP14 binds to the proteasome. In considering the homeostasis within the cell, we assume that the concentrations of S_{U2}, S_U, and U remain constant. In Fig 4A, the reaction network for USP14-regulated proteasomal substrate degradation in Fig 1C is simplified as the substrate degradation loop $PD \to PDS_{U2} \to PD_US_U^i \to PD_U \to PD$ coupled with the loop of deubiquitination $PD \to PDS_{U2} \to PD_US_U \to PD_U \to PD$.

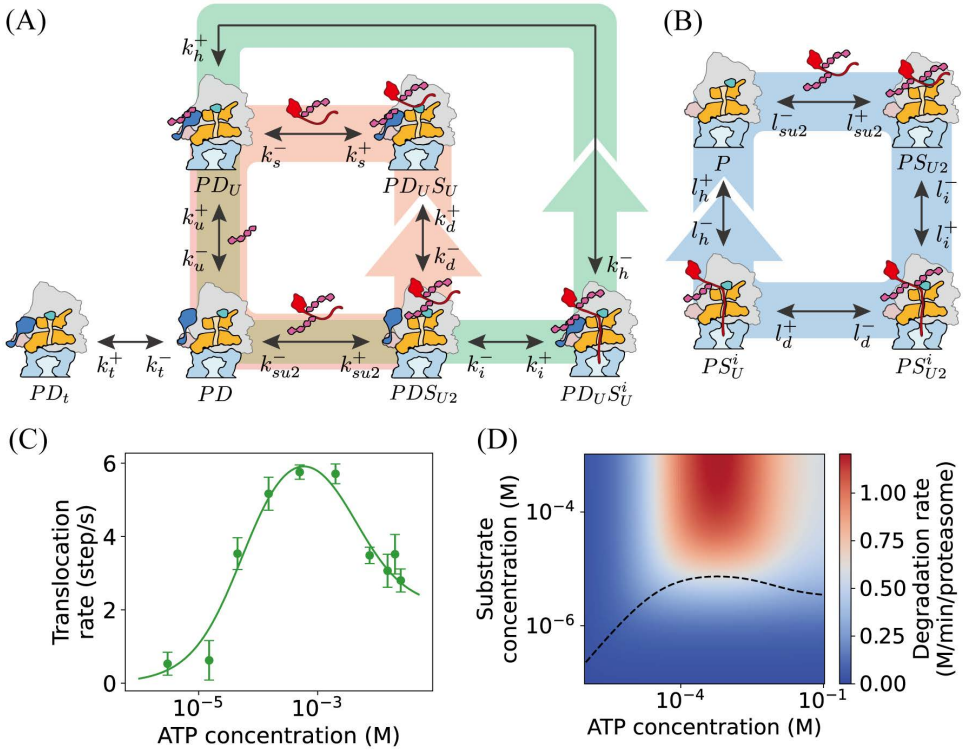

Fig 4. Simplified model and the influence of substrate and ATP on substrate degradation. (A) Simplification of the reaction network in Fig 1C for USP14-regulated proteasomal substrate degradation. Pink and green arrows represent the reaction loop for USP14-mediated deubiquitination and the loop for substrate degradation, respectively. (B) A simple reaction network of proteasomal substrate degradation free of USP14. Blue arrows indicate the loop of substrate degradation. (C) The experimentally observed substrate translocation rates (dots) [30] fitted with the formula of Eq. 5 (curve). (D) The dependence of substrate degradation rate on the concentrations of substrate and ATP predicted by Eqs. 3, 5 and 6. The black dashed line denotes the half-maximal effective concentration (EC_{50}) of the substrate under various ATP concentrations. The parameter values used are listed in Table B in S1 Text.

https://doi.org/10.1371/journal.pcbi.1012761.g004

In comparison, Fig 4B illustrates a simple loop of substrate degradation $P \to PS_{U2} \to PS^i_{U2} \to PS^i_U \to P$, in which the proteasome is not regulated by USP14. The kinetic equations of mass action law are assumed for the networks in Fig 4A and 4B and are given in Supporting information (Equations B and C in S1 Text) together with the parameters (Tables B and C in S1 Text).

The influence of USP14 on the rate of proteasomal substrate degradation can be obtained by analyzing the simplified model for USP14-regulated substrate degradation (Fig 4A) in comparison with the simple reaction model for the degradation without USP14 (Fig 4B). For both cases, the steady-state substrate degradation rates can be obtained analytically by setting the right-hand sides of Equations B and C in S1 Text to zero. In Fig 4B, the processes of substrate insertion, translocation and hydrolysis, deubiquitination, unbinding of ubiquitin and deubiquitinated substrate are nearly irreversible, the relevant parameters in Table C in S1 Text are negligible with $l_i^- = l_d^- = l_h^- \approx 0$. The substrate degradation rate v_{-USP14} for the USP14-free process can be deduced to be,

$$v_{-USP14} = l_h^+ \left[PS^i\right] = \frac{v_{m,-USP14}[P_t][S_{U2}]}{K_{-USP14}+[S_{U2}]}, \tag{1}$$

where l_h^+ is the rate of substrate hydrolysis, $[P_t]$ is the total concentration of all proteasomal states, $K_{-USP14} = \frac{l_d^+ l_h^+ (l_i^+ + l_{su2}^-)}{(l_h^+ l_i^+ + l_d^+ l_h^+ + l_d^+ l_i^+) l_{su2}^-}$, and $v_{m,-USP14}$ is the saturated rate,

$$v_{m,-USP14} = \frac{1}{\frac{1}{l_i^+}+\frac{1}{l_h^+}+\frac{1}{l_d^+}}. \tag{2}$$

Similarly, for the case of substrate degradation regulated by USP14 (Fig 4A), the relevant rate parameters in Table B in S1 Text for the negligible inverse reactions are assumed as zero with $k_i^- = k_d^- = k_h^- = k_u^- = k_s^+ \approx 0$, the substrate degradation rate v_{+USP14}, which is $k_h^+ \left[PD_U S_U^i\right]$, for USP14-regulated proteasomal degradation rate takes the form,

$$v_{+USP14} = \frac{v_{m,+USP14}[P_t][S_{U2}]}{K_{+USP14}+[S_{U2}]}, \tag{3}$$

in which, the saturated degradation rate is,

$$v_{m,+USP14} = \frac{1}{\frac{1}{k_i^+}+\frac{1}{k_h^+}+\frac{1}{k_u^-}+\frac{k_d^+}{k_i^+}\left(\frac{1}{k_u^-}+\frac{1}{k_s^-}\right)}, \tag{4}$$

and $K_{+USP14} = \frac{k_h^+ k_s^- k_u^- \left(k_d^+ + k_i^+ + k_{su2}^-\right)\left(k_t^- + k_t^+\right)}{k_{su2}^+ k_t^- \left(k_i^+ k_s^- k_u^- + k_h^+ k_s^- \left(k_i^+ + k_u^-\right) + k_d^+ k_h^+ \left(k_s^- + k_u^-\right)\right)}$.

The effect of USP14 on degradation can be obtained by checking the substrate degradation rates of Eq. 3 in comparison with Eq. 1. As the expressions of Eqs. 1 and 3 are complex, it is not convenient to evaluate the relative size of v_{-USP14} and v_{+USP14} to determine whether the influence of USP14 on the substrate degradation rate is positive or not. Take a step back, the saturated degradation rates $v_{m,-USP14}$ and $v_{m,+USP14}$ of Eqs. 2 and 4 can be compared due to their simpler forms. Typically, the processes of substrate insertion and hydrolysis are not influenced by the binding of USP14, thus $k_i^+ \approx l_i^+$ and $k_h^+ \approx l_h^+$. The parameter l_d^+ in Eq. 2 is the deubiquitination rate constant of RPN11 in the absence of USP14, and k_u^- in Eq. 4 is the rate constant for ubiquitin falling off USP14 in the presence of USP14. According to recent experiments, l_d^+ is from one to two orders of magnitude larger than k_u^- [7]. As l_d^+ in Eq. 2 is generally much greater than k_u^- in Eq. 4, it is always the case that $v_{m,+USP14} < v_{m,-USP14}$. Therefore, under conditions of substrate saturation, the typical effect of USP14 regulation is to reduce the rate at which substrates are degraded by the proteasome. The model result is consistent with the experimental findings that demonstrated USP14 inhibits the substrate degradation by the proteasome [23,25,27].

2.2.2 The dependency of the degradation rate on substrate and ATP concentrations for USP14-bound proteasome. The rate v_{+USP14} in Eq. 3 for USP14-regulated proteasomal protein degradation not only depends on the concentration of substrate $[S_{U2}]$, but also a function of the substrate hydrolysis rate k_h^+ which is determined by the concentration of ATP. Previous biochemical experiments have highlighted that the rate of substrate translocation in the proteasome doesn't rise monotonically with increasing ATP concentration [30]. As depicted in Fig 4C (dots), the rate follows a biphasic pattern. Initially, the rate increases as ATP concentration goes up, then paradoxically decreases at higher ATP levels. The experimental substrate translocation rate in (30) is found to be best fitted with the following Hill functional form (curve in Fig 4C):

$$r_{trans} = \frac{v_1[ATP]}{K_1+[ATP]} - \frac{v_2[ATP]}{K_2+[ATP]}. \tag{5}$$

Where $v_1 = 7.214\ \frac{step}{s}$, $v_2 = 5.165\ \frac{step}{s}$, $K_1 = 5.666 \times 10^{-5}\ M$, and $K_2 = 3.962 \times 10^{-3}\ M$. The rate of substrate hydrolysis depends linearly on the translocation rate,

$$k_h^+ = C \cdot r_{trans}, \tag{6}$$

where C is the coefficient. It is estimated here to be $0.307\frac{(M\cdot s)}{(\min\cdot step)}$ from the experimentally observed translocation rate in (30) under conditions of 1mM ATP and the hydrolysis rate k_h^+ we use in our simulations of Equations A in S1 Text.

The dependence of the USP14-regulated proteasomal hydrolysis rate on both substrate and ATP concentrations can be readily obtained by substituting Eq. 6 into Eq. 3. Fig 4D depicts the substrate degradation rate v_{+USP14} as the function of $[S_{U2}]$ and $[ATP]$ concentrations with the parameter values in Table B in S1 Text. The peak of the translocation rate does not appear in the upper-right corner of $[S_{U2}]$-$[ATP]$ space due to the biphasic relationship between the substrate translocation rate and ATP concentration. From Fig 4D, the range of ATP concentration for optimal degradation remains consistent for different substrate concentrations larger than 0.01 mM. Also illustrated in Fig 4D is the black dashed line denoting the half-maximal effective concentration (EC50) of the substrate across different ATP concentrations. EC50 is defined as the substrate concentration corresponding to half the maximum degradation rate at each ATP concentration. It rises as the ATP concentration increases, and then declines once the optimal ATP concentration has been exceeded. The EC50 curve represents the interplay between the ATPase motor's dynamics and other processes occurring in the proteasome bound by USP14, a relationship that can be verified through future experimental studies.

2.2.3 The influence of USP14 on substrate preference in proteasomal degradation. Within living cells, proteasomes frequently encounter the task of concurrently degrading multiple types of substrates. Given the distinct properties of these substrates, the degradation rates often differ significantly, and proteasomes exhibit preferences in the degradation of substrates [31]. The interplay between proteasomes and USP14 modulates the kinetics of substrate degradation, thereby would shape the selective preferences of the 26S proteasome towards various substrates. To investigate the influence of USP14 on substrate selectivity, we consider that two different substrates, denoted as S and T, are present in the reactions of Fig 4A and 4B. The reaction kinetic equations, for both with and without the regulation of USP14, are detailed in Supporting information (Equations D and E in S1 Text). The degradation preference of substrate S over substrate T can be quantified by the ratio of their respective degradation rates., *i.e.*, $P_{ST} = v_S/v_T$. The influence of USP14 on the substrate preference during degradation can be estimated by comparing the relative magnitudes of the preferences $P_{ST,+USP14}$ in the presence of USP14 and $P_{ST,-USP14}$ in its absence. It is reasonable to assume that USP14 would not influence substrate binding/unbinding and tail insertion into the proteasome, and the relevant rate constants for substrate S (k's) and substrate T (l's) are approximately equal (refer to Method). On this basis, the preference ratio $\eta \equiv P_{ST,+USP14}/P_{ST,-USP14}$ at the stationary state is found to be,

$$\eta = \frac{\left(1+\frac{k_{su2}^-}{k_{i,s}^+}\right)\left(1+\frac{k_{d,t}^+}{k_{i,t}^+}+\frac{k_{tu2}^-}{k_{i,t}^+}\right)}{\left(1+\frac{k_{tu2}^-}{k_{i,t}^+}\right)\left(1+\frac{k_{d,s}^+}{k_{i,s}^+}+\frac{k_{su2}^-}{k_{i,s}^+}\right)}, \tag{7}$$

where $k_{su2}^-, k_{d,s}^+, k_{i,s}^+$(and $k_{tu2}^-, k_{d,t}^+, k_{i,t}^+$,) are the rate constant of substrate unbinding, deubiquitination of USP14, and substrate insertion into the ATPase motor for S (and T). The rate constants of unbinding (k_{su2}^-/k_{tu2}^-), deubiquitination ($k_{d,s}^+/k_{d,t}^+$), and insertion ($k_{i,s}^+/k_{i,t}^+$) for substrate S relative to substrate T determine the preference ratio η in combination. For USP14 to enhance the degradation preference of substrate S, it is necessary that $\eta > 1$ or, equivalently.

$$\frac{k_{d,t}^+}{k_{i,t}^+ + k_{tu2}^-} > \frac{k_{d,s}^+}{k_{i,s}^+ + k_{su2}^-}. \tag{8}$$

In case $\eta = 1$, the above inequality holds with equality. The influence of USP14, quantified by Eq. 7, on the preferential degradation of substrate S over T is vividly depicted through the heat maps in Fig 5. The maps illustrate the relationship

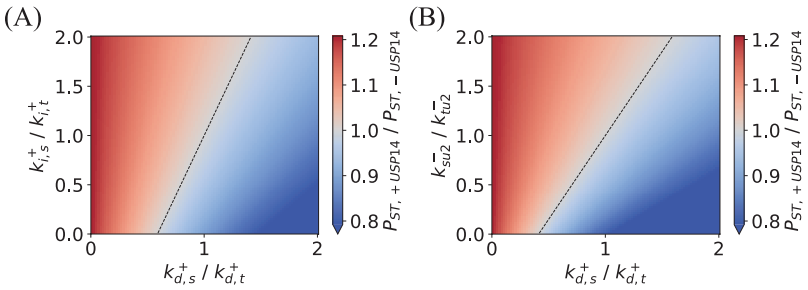

Fig 5. Effects of USP14 on substrate preference in proteasomal degradation. The preference ratio η in Eq. 8 is illustrated in the relative rate space $\frac{k^+_{i,s}}{k^+_{i,t}}$ versus $\frac{k^+_{d,s}}{k^+_{d,t}}$ (A), and in $\frac{k^-_{su2}}{k^-_{tu2}}$ versus $\frac{k^+_{d,s}}{k^+_{d,t}}$ space (B). The black dashed line indicates $\eta = 1$ where the degradation preferences of substrate *S* to *T* in USP14-bound and USP14-free proteasomes are equal. Parameters: $k^-_{su2} = k^-_{tu2} = 1.785 \times 10^{-1}\ s^{-1}$, $k^+_{i,t} = 10^{-3}\ s^{-1}$, $k^+_{d,t} = 6.364 \times 10^{-2}\ s^{-1}$ for (A), and $k^+_{i,s} = k^+_{i,t} = 10^{-3}\ s^{-1}$, $k^-_{tu2} = 1.785 \times 10^{-1}\ s^{-1}$, $k^+_{d,t} = 6.364 \times 10^{-2}\ s^{-1}$ for (B).

https://doi.org/10.1371/journal.pcbi.1012761.g005

in the relative rate space $\frac{k^+_{i,s}}{k^+_{i,t}}$ versus $\frac{k^+_{d,s}}{k^+_{d,t}}$ (Fig 5A), and further in the alternative relative rate space $\frac{k^-_{su2}}{k^-_{tu2}}$ plotted against $\frac{k^+_{d,s}}{k^+_{d,t}}$ (Fig 5B). The intermediate dividing line with $\eta = 1$ is marked. From Eqs. 7 and 8 and Fig 5, it can be concluded that with relatively large ratios of $\frac{k^-_{su2}}{k^-_{tu2}}$ or $\frac{k^+_{i,s}}{k^+_{i,t}}$, or small $\frac{k^+_{d,s}}{k^+_{d,t}}$ — in other words, when the substrate is easier to dissociate from the proteasome, or readily inserted into the OB-ring, or less sensitive to ubiquitination — its proteasomal degradation would be enhanced by the binding of USP14 to the proteasome.

3. Discussion

The ubiquitin-proteasome system (UPS), which includes USP14 and the 26S proteasome, is crucial for the regulation of protein turnover in cells. Studying their interaction provides insight into the mechanisms underlying protein degradation, which is fundamental to cellular homeostasis. The process of proteasome-mediated protein degradation occurs rapidly, with timescales on the order of milliseconds to seconds. Capturing intermediate states during this process is technically challenging due to the fast kinetics involved. The addition of USP14 introduces further complexity to its conformational changes. Distinguishing and classifying these dynamic states at high resolution requires sophisticated cryo-EM imaging analysis and classification algorithms. Up to now, time-resolved cryo-EM experiments on USP14-regulated allostery of the 26S proteasome are very limited, and an accurate understanding of the highly dynamic machine in substrate degradation remains elusive [27]. For instances, cryo-EM experiments have provided only fragmentary and vague views on the rapid conformational changes of the ATPase motor, and it is difficult to obtain cryo-EM images for substrate conformations outside the OB-ring due to its structural flexibility under thermal noise.

The limitations in experimental studies necessitate the use of mathematical modeling to hypothesize in experimental uncertainties and to gain complementary insights into the intricate substrate degradation process. This is particularly pertinent when detailed cryo-EM studies, aiming to capture time-resolved proteasomal allostery, are challenging to achieve. In this paper, we presented a kinetic model which is based on recent experimental findings in USP14-bound proteasomal conformations in substrate degradation. Our model accurately interpreted the recent experimental data on the time-resolved variations in the conformational landscape of human 26S proteasomes, as detailed in the study of [27]. Consistent with experimental findings, the model demonstrated that the proteasome's rate of substrate degradation is reduced under the regulatory influence of USP14. Our model illustrated how the rate of degradation is influenced by the concentrations of substrate and ATP, and it predicted the EC50 value of the substrate for varying ATP concentrations. When confronted with multiple substrates, USP14 influences the proteasome's preference, leading it to favor substrates

that can readily engage with the OB-ring, are weaker bound to the proteasome, and are less susceptible to deubiquitination processes.

The regulatory role of USP14 on the proteasome has been a focus in study of the USP14-proteasome complex. Several studies have demonstrated its inhibitory effect on substrate degradation [23,25,27]. It is important to note that the present experimental evidence is not comprehensive enough to definitively ascertain the inhibitory role of USP14 across the entire spectrum of substrates. Our model suggested that the inhibitory effect of USP14 depends on several parameters that are rooted in the structural characteristics of the substrate. Theoretically, there might exist a class of substrates upon which USP14 could have a facilitative impact. In fact, USP14 has been recently found to exert activating effects on the proteasome [32]. It was reported that if the proteasome binds to USP14 with only the UBL domain, it can up-regulate the degradation rate of substrates by the proteasome. The precise mechanism underlying the heightened degradation rate observed with the UBL-domain-only USP14 remains unclear. As such an incomplete USP14 does not exist under *in vivo* conditions, the observation may not apply to the case of complete USP14 with both UBL and USP domains. In fact, the absence of the USP domain in the truncated form prevents USP14 from executing its deubiquitinating function on substrates. The regulation of USP14 without the USP domain to the 26S proteasome might be very different from the situation we considered here. To date, there have been no experimental reports indicating that complete USP14 can achieve an increase in degradation rates.

Experimental findings regarding substrate preference and selectivity of the 26S proteasome in substrate degradation have been accumulated. Several factors have been revealed that can influence the substrate selectivity, including the amino acid sequence and the length of the initiation region of substrate [33–36], the number of ubiquitin chains, as well as the position, length, and type of each ubiquitin chain [31,37]. The specific role of USP14 in altering proteasomal substrate selectivity is still unclear. Our model analyses suggest that a substrate, when compared to others, which is more readily inserted into the OB-ring and easily disengaged from the proteasome, while simultaneously being less susceptible to deubiquitination by USP14, would be preferentially targeted for degradation by the proteasome complexed with USP14. This provides a fresh perspective on the potential biological roles of USP14 and encourages further experimental exploration to better understand its functions.

4. Method

In the simulations of Equations A in S1 Text, the ordinary differential equations are numerically solved and analyzed using Python SciPy (version 1.7.3) and NumPy library (version 1.22.4). We assume that before the addition of substrate, the transition between the USP14-bound proteasome *PD* state and the PD_t state, in which the entry to the OB-ring is blocked by RPN11, is at equilibrium. In accordance with the experimental setup [27], we set the initial concentrations for *PD*, PD_t, and S_{U2} as $[PD]_0 = 0.949\ \mu M$, $[PD_t]_0 = 0.051\ \mu M$, $[S_{U2}]_0 = 10\ \mu M$, while all other variables are initialized to zero. The rate constants for substrate binding and dissociation from the proteasome, as well as those for substrate insertion and translocation in the ODEs of Equations A in S1 Text, can be adopted from experimental measurements [6,30,31]. Since these experiments were conducted at temperatures higher than those of the time-resolved cryo-EM experiments (below 10 °C), we use the experimentally measured rates as upper bounds for fitting. The remaining rate constants have no upper bounds and are free to vary during fitting. The rate constants were determined by fitting the simulation results to the time-resolved cryo-EM experimental data in Fig 3A, including the proportions of E_A-like, E_D-like, and S_D-like categories of conformation, as well as the concentration of residual substrate relative to the initial amount. The full parameter values and the settings of upper bounds during fitting for Equations A in S1 Text are listed in Supporting information (Table A in S1 Text). We also conduct a parameter sensitivity analysis (Fig A in S1 Text), which highlights the critical roles of the substrate binding rate, tail insertion rate, deubiquitination rate, and substrate translocation hydrolysis rate in USP14-mediated regulation of proteasomal processes. In our simulations of the temporal changes in

the percentage populations of 13 intermediate conformations of the USP14-bound proteasome (shown in Fig 3B–3D), we assume that quasi-equilibriums have been achieved within the E_A-like, E_D-like, and S_D-like classes during substrate degradation. While the concentrations in each class undergo temporal changes, the ratios between them should remain roughly constant. In our simulations, the fixed ratios are determined by fitting the model results to the experimental observations.

To evaluate the effects of USP14 on proteasomal degradation and substrate preferences, we adopt the simplified model in Fig 4A and compare it to the scenario depicted in Fig 4B, which lacks USP14. The kinetic equations for the reaction networks in Fig 4A and 4B are listed in Supporting information (Equations B and C in S1 Text), with rate constants denoted differently by k's and l's, respectively. For both USP14-free and USP14-bound proteasomes, we use identical concentrations of proteasome, substrate, and ATP at the same temperature in our analyses to compare the degradation processes. We also assume that the influences of USP14 on substrate binding and release, tail insertion, and translocation and hydrolysis rates can be disregard, *i.e.*, $k_i^+ \approx l_i^+, k_h^+ \approx l_h^+, k_{su2}^+ \approx l_{su2}^+$ in considering the effect of USP14 on proteasome degradation rates. Similarly, when assessing the effect of USP14 on proteasome substrate preference, $k_{su2}^+ \approx l_{su2}^+,\ k_{\overline{su2}} \approx l_{\overline{su2}},\ k_{tu2}^+ \approx l_{tu2}^+,\ k_{\overline{tu2}} \approx l_{\overline{tu2}}, k_{i,s}^+ \approx l_{i,s}^+, k_{i,t}^+ \approx l_{i,t}^+$ are assumed.

The expression of η (Eq. 7) is derived from the steady-state of Eqs. 4 and 5. The preference of substrate S over substrate T in USP14-regulated proteasomal degradation, which is calculated as $\frac{k_{h,s}^+[PD_US_U^i]}{k_{h,t}^+[PD_UT_U^i]}$, is determined and given by,

$$P_{ST,+USP14} = \frac{k_{su2}^+\left(1+\frac{k_{d,t}^+}{k_{i,t}^+}+\frac{k_{\overline{tu2}}}{k_{i,t}^+}\right)}{k_{tu2}^+\left(1+\frac{k_{d,s}^+}{k_{i,s}^+}+\frac{k_{\overline{su2}}}{k_{i,s}^+}\right)} \cdot \frac{[S_{U2}]}{[T_{U2}]}. \tag{9}$$

For the case of USP14-free degradation, the preference, which is equal to $\frac{l_{h,s}^+[PS_U^i]}{l_{h,t}^+[PT_U^i]}$, has the form,

$$P_{ST,-USP14} = \frac{l_{su2}^+\left(1+\frac{l_{\overline{tu2}}}{l_{i,t}^+}\right)}{l_{tu2}^+\left(1+\frac{l_{\overline{su2}}}{l_{i,s}^+}\right)} \cdot \frac{[S_{U2}]}{[T_{U2}]}, \tag{10}$$

where k_{su2}^+ and $k_{\overline{su2}}$ (and l_{tu2}^+ and $l_{\overline{tu2}}$) are the rate constants for binding and unbinding of ubiquitin-tagged substrate S_{U2} (and T_{U2}) to the proteasome, with subscripts 's' and 't' for substrate S and substrate T, respectively. The magnitudes of $P_{ST,+USP14}$ and $P_{ST,-USP14}$ in Eqs. 9 and 10 depend on the parameters k's and l's. The ratio of Eqs. 9 and 10 gives the equation for η (Eq. 7). Inequality Eq. 8 is deduced from expression Eq. 7 by letting $\eta > 1$.

Supporting information

S1 Text. Supporting information, including Text A, Table A–C, Equations A–E and Figure A.
(DOCX)

Author contributions

Conceptualization: Qi Ouyang, Hongli Wang, Youdong Mao.

Formal analysis: Di Wu, Hongli Wang.

Funding acquisition: Qi Ouyang, Hongli Wang, Youdong Mao.

Investigation: Di Wu.

Methodology: Di Wu, Qi Ouyang, Hongli Wang, Youdong Mao.

Software: Di Wu.

Supervision: Qi Ouyang, Hongli Wang, Youdong Mao.

Validation: Di Wu, Hongli Wang.

Visualization: Di Wu.

Writing – original draft: Di Wu.

Writing – review & editing: Di Wu, Hongli Wang.

References

1. Bard JAM, Goodall EA, Greene ER, Jonsson E, Dong KC, Martin A. Structure and function of the 26S proteasome. Annu Rev Biochem. 2018;87:697–724. https://doi.org/10.1146/annurev-biochem-062917-011931 PMID: 29652515
2. Mao Y. Structure, dynamics and function of the 26S proteasome. In: Macromolecular protein complexes III: Structure and function; 2021. p. 1–151.
3. Dong Y, Zhang S, Wu Z, Li X, Wang WL, Zhu Y, et al. Cryo-EM structures and dynamics of substrate-engaged human 26S proteasome. Nature. 2019;565(7737):49–55. https://doi.org/10.1038/s41586-018-0736-4 PMID: 30479383
4. Beckwith R, Estrin E, Worden EJ, Martin A. Reconstitution of the 26S proteasome reveals functional asymmetries in its AAA+ unfoldase. Nat Struct Mol Biol. 2013;20(10):1164–72. https://doi.org/10.1038/nsmb.2659 PMID: 24013205
5. Greene ER, Goodall EA, de la Peña AH, Matyskiela ME, Lander GC, Martin A. Specific lid-base contacts in the 26s proteasome control the conformational switching required for substrate degradation. Elife. 2019;8:e49806. https://doi.org/10.7554/eLife.49806 PMID: 31778111
6. Bard JAM, Bashore C, Dong KC, Martin A. The 26S proteasome utilizes a kinetic gateway to prioritize substrate degradation. Cell. 2019;177(2):286-298.e15. https://doi.org/10.1016/j.cell.2019.02.031 PMID: 30929903
7. Jonsson E, Htet ZM, Bard JAM, Dong KC, Martin A. Ubiquitin modulates 26S proteasome conformational dynamics and promotes substrate degradation. Sci Adv. 2022;8(51):eadd9520. https://doi.org/10.1126/sciadv.add9520 PMID: 36563145
8. Albert S, Schaffer M, Beck F, Mosalaganti S, Asano S, Thomas HF, et al. Proteasomes tether to two distinct sites at the nuclear pore complex. Proc Natl Acad Sci U S A. 2017;114(52):13726–31. https://doi.org/10.1073/pnas.1716305114 PMID: 29229809
9. Chen S, Wu J, Lu Y, Ma Y-B, Lee B-H, Yu Z, et al. Structural basis for dynamic regulation of the human 26S proteasome. Proc Natl Acad Sci U S A. 2016;113(46):12991–6. https://doi.org/10.1073/pnas.1614614113 PMID: 27791164
10. de la Peña AH, Goodall EA, Gates SN, Lander GC, Martin A. Substrate-engaged 26S proteasome structures reveal mechanisms for ATP-hydrolysis-driven translocation. Science. 2018;362(6418):eaav0725. https://doi.org/10.1126/science.aav0725 PMID: 30309908
11. Verma R, Chen S, Feldman R, Schieltz D, Yates J, Dohmen J, et al. Proteasomal proteomics: identification of nucleotide-sensitive proteasome-interacting proteins by mass spectrometric analysis of affinity-purified proteasomes. Mol Biol Cell. 2000;11(10):3425–39. https://doi.org/10.1091/mbc.11.10.3425 PMID: 11029046
12. Wang X, Chen C-F, Baker PR, Chen P, Kaiser P, Huang L. Mass spectrometric characterization of the affinity-purified human 26S proteasome complex. Biochemistry. 2007;46(11):3553–65. https://doi.org/10.1021/bi061994u PMID: 17323924
13. Guerrero C, Tagwerker C, Kaiser P, Huang L. An integrated mass spectrometry-based proteomic approach: quantitative analysis of tandem affinity-purified in vivo cross-linked protein complexes (QTAX) to decipher the 26 S proteasome-interacting network. Mol Cell Proteomics. 2006;5(2):366–78. https://doi.org/10.1074/mcp.M500303-MCP200 PMID: 16284124
14. Borodovsky A, Kessler B, Casagrande R, Overkleeft H, Wilkinson K, Ploegh H. A novel active site-directed probe specific for deubiquitylating enzymes reveals proteasome association of USP14. EMBO J. 2001;20(18):5187–96.
15. Hamazaki J, Iemura S-I, Natsume T, Yashiroda H, Tanaka K, Murata S. A novel proteasome interacting protein recruits the deubiquitinating enzyme UCH37 to 26S proteasomes. EMBO J. 2006;25(19):4524–36. https://doi.org/10.1038/sj.emboj.7601338 PMID: 16990800
16. Qiu X-B, Ouyang S-Y, Li C-J, Miao S, Wang L, Goldberg AL. hRpn13/ADRM1/GP110 is a novel proteasome subunit that binds the deubiquitinating enzyme, UCH37. EMBO J. 2006;25(24):5742–53. https://doi.org/10.1038/sj.emboj.7601450 PMID: 17139257
17. Yao T, Song L, Xu W, DeMartino GN, Florens L, Swanson SK, et al. Proteasome recruitment and activation of the Uch37 deubiquitinating enzyme by Adrm1. Nat Cell Biol. 2006;8(9):994–1002. https://doi.org/10.1038/ncb1460 PMID: 16906146
18. Crosas B, Hanna J, Kirkpatrick DS, Zhang DP, Tone Y, Hathaway NA, et al. Ubiquitin chains are remodeled at the proteasome by opposing ubiquitin ligase and deubiquitinating activities. Cell. 2006;127(7):1401–13.
19. Leggett DS, Hanna J, Borodovsky A, Crosas B, Schmidt M, Baker RT, et al. Multiple associated proteins regulate proteasome structure and function. Mol Cell. 2002;10(3):495–507. https://doi.org/10.1016/s1097-2765(02)00638-x PMID: 12408819
20. Sakata E, Yamaguchi Y, Kurimoto E, Kikuchi J, Yokoyama S, Yamada S, et al. Parkin binds the Rpn10 subunit of 26S proteasomes through its ubiquitin-like domain. EMBO Rep. 2003;4(3):301–6. https://doi.org/10.1038/sj.embor.embor764 PMID: 12634850

21. Martínez-Noël G, Galligan JT, Sowa ME, Arndt V, Overton TM, Harper JW, et al. Identification and proteomic analysis of distinct UBE3A/E6AP protein complexes. Mol Cell Biol. 2012;32(15):3095–106. https://doi.org/10.1128/MCB.00201-12 PMID: 22645313
22. Kühnle S, Martínez-Noël G, Leclere F, Hayes SD, Harper JW, Howley PM. Angelman syndrome-associated point mutations in the Zn2+-binding N-terminal (AZUL) domain of UBE3A ubiquitin ligase inhibit binding to the proteasome. J Biol Chem. 2018;293(47):18387–99. https://doi.org/10.1074/jbc.RA118.004653 PMID: 30257870
23. Hanna J, Hathaway NA, Tone Y, Crosas B, Elsasser S, Kirkpatrick DS, et al. Deubiquitinating enzyme Ubp6 functions noncatalytically to delay proteasomal degradation. Cell. 2006;127(1):99–111. https://doi.org/10.1016/j.cell.2006.07.038 PMID: 17018280
24. Aufderheide A, Beck F, Stengel F, Hartwig M, Schweitzer A, Pfeifer G, et al. Structural characterization of the interaction of Ubp6 with the 26S proteasome. Proc Natl Acad Sci U S A. 2015;112(28):8626–31. https://doi.org/10.1073/pnas.1510449112 PMID: 26130806
25. Lee B-H, Lu Y, Prado MA, Shi Y, Tian G, Sun S, et al. USP14 deubiquitinates proteasome-bound substrates that are ubiquitinated at multiple sites. Nature. 2016;532(7599):398–401. https://doi.org/10.1038/nature17433 PMID: 27074503
26. Hung KYS, Klumpe S, Eisele MR, Elsasser S, Tian G, Sun S, et al. Allosteric control of Ubp6 and the proteasome via a bidirectional switch. Nat Commun. 2022;13(1):838. https://doi.org/10.1038/s41467-022-28186-y PMID: 35149681
27. Zhang S, Zou S, Yin D, Zhao L, Finley D, Wu Z, et al. USP14-regulated allostery of the human proteasome by time-resolved cryo-EM. Nature. 2022;605(7910):567–74. https://doi.org/10.1038/s41586-022-04671-8 PMID: 35477760
28. Shi Y, Chen X, Elsasser S, Stocks B, Tian G, Lee B, et al. Rpn1 provides adjacent receptor sites for substrate binding and deubiquitination by the proteasome. Science. 2016;351(6275):aad9421.
29. Bashore C, Dambacher CM, Goodall EA, Matyskiela ME, Lander GC, Martin A. Ubp6 deubiquitinase controls conformational dynamics and substrate degradation of the 26S proteasome. Nat Struct Mol Biol. 2015;22(9):712–9. https://doi.org/10.1038/nsmb.3075 PMID: 26301997
30. Fang R, Hon J, Zhou M, Lu Y. An empirical energy landscape reveals mechanism of proteasome in polypeptide translocation. Elife. 2022;11:e71911. https://doi.org/10.7554/eLife.71911 PMID: 35050852
31. Lu Y, Lee B, King RW, Finley D, Kirschner MW. Substrate degradation by the proteasome: a single-molecule kinetic analysis. Science. 2015;348(6231):1250834. https://doi.org/10.1126/science.1250834 PMID: 25859050
32. Kim HT, Goldberg AL. UBL domain of Usp14 and other proteins stimulates proteasome activities and protein degradation in cells. Proc Natl Acad Sci U S A [Internet]. 2018 [cited 2024 Apr 15];115(50):E11642–50. Available from: https://pnas.org/doi/full/10.1073/pnas.1808731115 PMID: 30487212
33. Inobe T, Fishbain S, Prakash S, Matouschek A. Defining the geometry of the two-component proteasome degron. Nat Chem Biol. 2011;7(3):161–7. https://doi.org/10.1038/nchembio.521 PMID: 21278740
34. Fishbain S, Prakash S, Herrig A, Elsasser S, Matouschek A. Rad23 escapes degradation because it lacks a proteasome initiation region. Nat Commun. 2011;2:192. https://doi.org/10.1038/ncomms1194 PMID: 21304521
35. Fishbain S, Inobe T, Israeli E, Chavali S, Yu H, Kago G, et al. Sequence composition of disordered regions fine-tunes protein half-life. Nat Struct Mol Biol. 2015;22(3):214–21. https://doi.org/10.1038/nsmb.2958 PMID: 25643324
36. Yu H, Singh Gautam AK, Wilmington SR, Wylie D, Martinez-Fonts K, Kago G, et al. Conserved sequence preferences contribute to substrate recognition by the proteasome. J Biol Chem. 2016;291(28):14526–39. https://doi.org/10.1074/jbc.M116.727578 PMID: 27226608
37. Yu H, Matouschek A. Recognition of client proteins by the proteasome. Annu Rev Biophys. 2017;46(1):149–73.